
OCTOBER
14-17
MWP 2025
International Topical Meeting
on Microwave Photonics
Centre des Congrès de Québec, Canada
mwp2025.org
Program

STUDENT AWARDS SPONSORS - COMMANDITAIRES PRIX ÉTUDIANTS

INRS Institut national de la recherche scientifique

COPL Centre d'optique, photonique et lasers

STARaCom

COOOPERATING ORGANIZATIONS - ORGANISATIONS PARTENAIRES

IEEE Photonics Society ESTABLISHED 1965

IEEE

MTT-S

EIC

IEEE Section de Québec

IEEE MONTRÉAL

COFFEE BREAKS SPONSOR - PARTENAIRE DES PAUSES-CAFÉ

Ansys / OPTICS

PROGRAM AD SPONSORS - PARTENAIRES PUBLICITÉ PROGRAMME

O/E LAND INC.

ANT APPLIED NANOTOOLS INC.

Tuesday, October 14, 2025 - Mardi le 14 octobre 2025		Room / Salle
12:00 - 18:45	Registration - Inscription Welcome Desk	Urban Space
13:00 - 15:00	Workshop 1 - New frontiers in neuromorphic photonics	309AB
15:00 - 15:30	Coffee Break - Pause-café	Urban Space
15:30 - 18:30	Workshop 2 - Photonic control of antennas	309AB

Wednesday, October 15, 2025 - Mercredi le 15 octobre 2025		Room / Salle
07:00 - 20:00	Registration - Inscription Welcome Desk	Urban Space
08:15 - 10:00	Welcome and Plenary Session 1	309AB
10:00 - 10:30	Coffee Break - Pause-café	Urban Space
10:30 - 12:15	We1 - Photonic microwave processing, sensing, and measurements 1	309AB
12:15 - 13:30	Lunch (included) - Repas du midi (inclus)	Urban Space
13:30 - 15:15	We2 - High-speed photomixers and optoelectronic converters and Tutorial	309AB
15:15 - 16:45	Coffee Break and We3 - Poster Session 1	Urban Space
16:45 - 18:25	We4 - High-performance microwave photonic signal sources 1	309AB
18:30 - 20:30	Welcome Reception - Réception de bienvenue	Urban Space

Thursday, October 16, 2025 - Jeudi le 16 octobre 2025		Room / Salle
08:00 - 18:30	Registration - Inscription Welcome Desk	Urban Space
08:30 - 10:00	Plenary Session 2 and Invited	309AB
10:00 - 10:30	Coffee Break - Pause-café	Urban Space
10:30 - 12:15	Th1 - Photonic-enhanced artificial intelligence (AI) computing techniques	309AB
12:15 - 13:30	Lunch (included) - Repas du midi (inclus)	Urban Space
13:30 - 15:00	Th2 - Integrated microwave photonics	309AB
15:15 - 16:45	Coffee Break and Th3 - Poster Session 2	Urban Space
16:45 - 18:15	Th4 - Radio over Fiber (RoF) for B5G/6G mobile data and terrestrial communication systems	309AB
18:30 - 21:30	Award Banquet Evening - Banquet de remise de prix	Monastère des Augustines

Friday, October 17, 2025 - Vendredi le 17 octobre 2025		Room / Salle
08:00 - 16:30	Registration - Inscription Welcome Desk	Urban Space
08:30 - 10:00	Plenary Session 3 and Invited	309AB
10:00 - 10:30	Coffee Break - Pause-café	Urban Space
10:30 - 12:15	Fr1 - High-performance microwave photonic signal sources 2	309AB
12:15 - 13:30	Lunch (included) - Repas du midi (inclus)	Urban Space
13:30 - 15:00	Fr2 - Photonic microwave processing, sensing, and measurements 2	309AB
15:00 - 15:30	Coffee Break - Pause-café	Urban Space
15:30 - 16:15	Fr3 - Postdeadline Session and Wrap-Up	309AB

POSTER PRESENTATIONS - PRÉSENTATIONS D'AFFICHES

Wednesday, October 14 - Mercredi 14 octobre

COFFEE BREAK AND WE3 - POSTER SESSION 1

15:15 - 16:45 CCQ URBAN SPACE VIA HALL 310

TERAHERTZ POLARIMETRIC SPECTROMETER USING CMOS DETECTOR
Redwan Ahmad, École de technologie supérieure (ÉTS), Canada
Redwan Ahmad, Xavier Ropagnol, Richard Al Hadi, François Blanchard
POSTER BOARD #01

Y-BRANCH WAVEGUIDE-TYPE EXCLUSIVE OR LOGICAL GATE FOR THZ-BAND COMMUNICATION
Koichi Takiguchi, Ritsumeikan University, Japan
Koichi Takiguchi, Wataru Ishihara
POSTER BOARD # 03

MICROWAVE PHOTONIC CHANNELIZATION-BASED BROADBAND PHASED ARRAY RECEIVER
Shilong Chen, Beijing University of Posts and Telecommunications, China (People's Republic of)
Shilong Chen
POSTER BOARD # 05

POWER RESPONSE OF GAINAS/INP UNI-TRAVELING CARRIER PHOTODIODES (UTC-PDS) WITH ABRUPT AND GRADED COLLECTORS
Amirmohammad Miran zadeh, ETH zurich, Switzerland
Amirmohammad Miran zadeh, Nikolaos Poumpouridis, Rinchen Bhutia, Pascal Kaufmann, Olivier Ostinelli, Colombo Bolognesi
Student Award finalist
POSTER BOARD # 07

A HIGHLY LINEAR AND COMPACT SI RING-ASSISTED MACH-ZEHNDER MODULATOR AT X BAND
Min-Hyeok Seong, Yonsei University, Korea, Republic of (South Korea)
Min-Hyeok Seong, Yongjin Ji, Woo-Young Choi
Student Award finalist
POSTER BOARD # 09

FAST TUNABLE INP-LNOI DBR LASER AT 1550NM
Sara Bassil, III-V Lab, France
Sara Bassil, Sylvain Boust, Cosimo Calo, Romain Hersent, Hamed Sattari, Ivan Prieto Gonzalez, Homa Zarebidaki, François Duport, Frédéric Van Dijk, Nadege Courjal
POSTER BOARD # 11

A PRACTICAL DEMONSTRATION OF MACH-ZEHNDER MODULATOR CHIRP MEASUREMENT USING A DC METHOD

Lam Bui, Central Queensland University (CQUniversity), Australia

Lam Bui

POSTER BOARD # 13

A 4.5 GHZ OPTICAL RECEIVER UTILIZING AN 800UW MODIFIED RGC TRANSIMPEDANCE AMPLIFIER

Jeongyong Yang, University of Virginia, United States of America

Shadrach Sarpong, Jeongyong Yang, Junwu Bai, Andreas Beling, Travis Blalock, Steven Bowers

POSTER BOARD # 15

MILLIMETER-WAVE FIXED WIRELESS: CHALLENGES AND INSIGHTS FROM MODELS AND MACHINE LEARNING

Ukrit Mankong, CHIANG MAI UNIVERSITY, Thailand

Nutwipa Pinkhumpee, Chumphon Kaewmalee, Ukrit Mankong

POSTER BOARD # 17

SELF-PULSATING III-V/SI DFB LASER FOR TUNABLE PHOTONIC MICROWAVE GENERATION

Mourad Azhar, SAMOVAR, Télécom SudParis, Institut Polytechnique de Paris, France

Mourad Azhar, Youcef Driouche, Joan Manel Ramirez, Kamel Merghem

POSTER BOARD # 19

PHOTONIC TERAHERTZ VECTOR ANALYSIS WITH OPTICAL FREQUENCY COMB MODULATION

Ding Zhe, Zhejiang University, Republic of China

Ding Zhe, Yang Zuomin, Lyu Zhidong, Chen Shiping, Zhou Peiqi, Zhang Lu, Yu Xianbin

POSTER BOARD # 21

A COST-EFFECTIVE SINGLE ELEMENT DIELECTRIC ROD ANTENNA FOR THZ APPLICATIONS

Guillermo Carpintero, Universidad Carlos III de Madrid, Spain

Asrin Piroutiniya, Muhsin Ali, Ashish Kumar, Alejandro Rivera-Lavado, David de Felipe, Lars Liebermeister, Philipp Winklhofer, Guillermo Carpintero

POSTER BOARD # 25

INTEGRATED THIN-FILM LITHIUM NIOBATE RECEIVER FOR BOTH FREQUENCY DEMULTIPLEXING AND MODULATION DE-CHIRPING FUNCTIONS IN DUAL-BAND RADAR

Fang Zou, Tianfu Xinglong Lake Laboratory, China (People's Republic of)

Yongtao Du, Ningyuan Zhong, Xihua Zou, Fang Zou, Wenlin Bai, Xiaojun Xie, Wei Pan, Lianshan Yan

POSTER BOARD # 27

A Highly Linear and Compact Si Ring-Assisted Mach-Zehnder Modulator at X Band

Min-Hyeok Seong
Department of Electrical and Electronic Engineering
Yonsei University
Seoul, Republic of Korea
alsguree@yonsei.ac.kr

Yongjin Ji
Department of Electrial and Electronic Engineering
Yonsei University
Seoul, Republic of Korea
yjji0314@yonsei.ac.kr

Woo-Young Choi
Department of Electrial and Electronic Engineering
Yonsei University
Seoul, Republic of Korea
wchoi@yonsei.ac.kr

***Abstract*— We demonstrate a Si ring-assisted Mach-Zehnder modulator (RAMZM) that achieves high spurious-free dynamic range (SFDR) at X band. The Si RAMZM has suppressed 3rd- and 5th-order intermodulation distortions (IMDs), resulting in a dominant 7th-order IMD component. The measured SFDR is 105.4 dB.Hz$^{6/7}$ at 10 GHz. The Si RAMZM also has a small footprint of only about 1 mm^2. These results highlight its potential for analog photonic applications.**

Keywords*— *Si photonics, ring-assisted Mach-Zehnder modulator, modulation linearity, spurious-free dynamic range

I. Introduction

Electro-optical (EO) modulators play a pivotal role in microwave photonic systems by enabling the conversion of electrical signals into the optical domain for high-speed and broadband signal processing. Among various modulator technologies, lithium niobate ($LiNbO_3$) based Mach–Zehnder modulators (MZMs) have long been the standard due to their excellent linearity and high electro-optic efficiency. However, with the increasing demand for compact, high-performance, and scalable microwave photonic systems, there is a growing shift toward the integration of EO modulators with other optical components. Such integration can provide the enhanced performance with reduced system footprint, power consumption, and cost.

Silicon photonics has emerged as a promising platform for photonic integration, offering the ability to fabricate photonic components using the same process technologies as electronic integrated circuits. This compatibility opens the door for large-scale integration and mass production. Nonetheless, silicon-based EO modulators—primarily relying on carrier-depletion mechanisms in silicon waveguides—suffer from poor linearity compared to their $LiNbO_3$ counterparts. This nonlinearity poses a significant challenge for microwave photonics applications, where linear signal modulation is essential.

To address this limitation, several linearization techniques have been proposed. These include electronic pre-distortion circuits [1] and third-order intermodulation distortion (IMD) cancellation methods [2], both of which attempt to compensate for the modulator's nonlinear response in the electrical domain. However, such techniques are inherently narrowband and fail to exploit the intrinsic broadband potential of photonic systems. Therefore, linearization method without electronic technique is necessary for microwave photonic systems. Attempts have been made for realizing with modified MZM structures. A dual-parallel MZM (DPMZM) has been reported that can greatly enhanced the spurious-free dynamic range (SFDR) [3]. However, the DPMZM has two MZMs, inevitably resulting in a large footprint. Recently, the Si ring-assisted Mach–Zehnder modulator (RAMZM) has been explored as a promising photonic-domain solution to this problem [4]. With the help of Si ring modulators (RMs), the Si RAMZM can be realized with a small footprint, which is of great advantage for photonic integration. In a Si RAMZM, the highly nonlinear voltage-to-phase response of a ring resonator is employed to counteract the compressive phase-to-intensity transfer function of the Si MZM, thereby improving linearity. However, the previously reported Si RAMZMs have a limited SFDR [4] or low operation frequency [5]. In this paper, we present a Si-based RAMZM that exhibits high linearity at X band.

II. Design, Fabrication and Characteristics

We fabricated the Si RAMZM using the multi-project wafer service offered by Advanced Micro Foundry. Fig. 1(a) shows a photograph of the fabricated device, and Fig. 1(b) presents its schematic diagram. The Si RAMZM adopts a Mach-Zehnder interferometer (MZI) architecture, where each arm of the MZI contains a RM implemented using multimode interferometers (MMIs). Light is coupled in and out of the chip through grating couplers. To enable monitoring of the optical signal from each RM, additional waveguides are integrated into each arm of the MZI. Moreover, each arm is equipped with a thermo-optic heater that allows fine control of MZI's optical bias via thermal tuning. The optical bias should be set to the quadrature point of the MZI transmission characteristic with the thermo-optic heaters. The total footprint of the Si RAMZM is approximately 1.45 mm × 0.7 mm. To adjust the operating point of the RM, a thermo-optic heater is embedded within each RM. A tunable coupler is located on one side of each RM, using a 2 × 2 MZI-based thermo-optic switch. The coupling coefficient κ between the through port and the ring waveguide can be controlled with

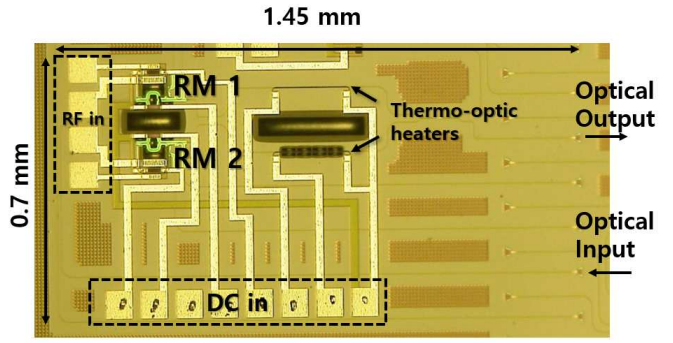

(a)

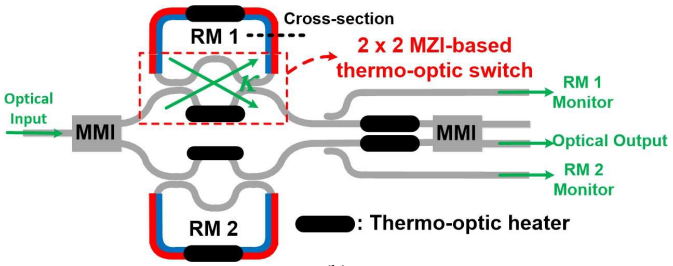

(b)

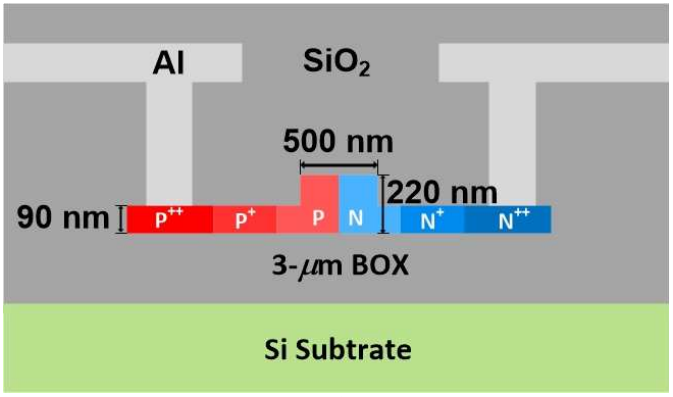

(c)

Fig. 1. (a) Chip photograph of the Si RAMZM, (b) Si RAMZM schematic, and (c) cross-section view of the RM

this tunable coupler. The two RMs incorporated in the Si RAMZM are of the depletion type. Fig. 1(c) depicts the cross-sectional view of the RM. The Si RAMZM employs a differential modulation scheme with two RMs. Differential modulation for RAMZM is known to improve linearity due to the cancellation of even-order harmonics in the phase response of the RM [5].

Fig. 2 illustrates the transmission characteristics of two RMs measured using the monitoring RM ports. The resonance wavelength and the coupling coefficient for both RMs are tuned such that their transmission characteristics are nearly identical. The estimated κ for each RM is about 0.61. For modulation, the RM resonance wavelength is used as the input wavelength as this provides the highest modulation efficiency and SFDR.

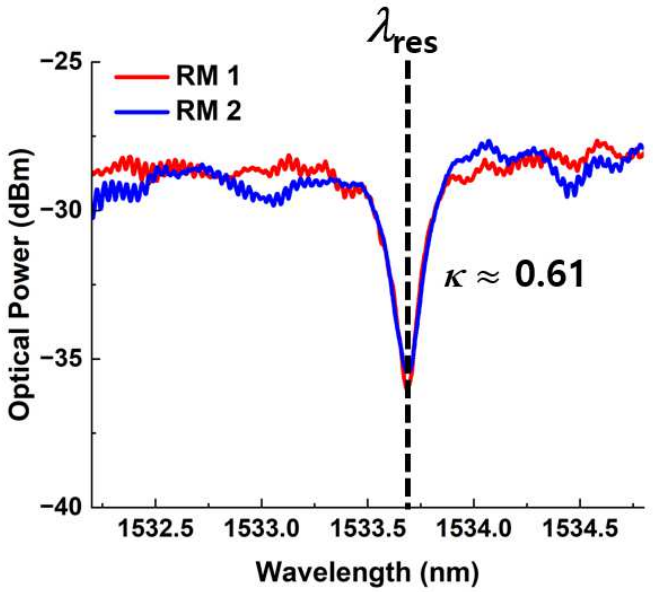

Fig. 2. The measured transmission characteristics along wavelength of the two RMs in Si RAMZM for differential modulation mode.

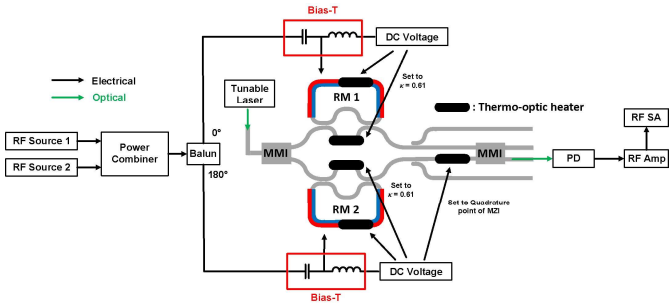

(a)

Fig. 3. Experimental setup for two-tone measurement. PD: photodetector, RF Amp: RF amplifier, RF SA: RF signal analyzer

III. Si RAMZM Linearity Measurement

To experimentally evaluate the linearity of the Si RAMZM, we performed two-tone measurements by injecting an microwave signal composed of two distinct frequencies and analyzing the output. The SFDR is determined by measuring the power of the fundamental tone and the closest IMD component from the fundamental tone. Fig. 3 shows the experimental setup for the two-tone measurement. Optical signal is provided by a tunable laser. Two RF sources are used for microwave signal generation and their outputs are combined with an RF combiner. For differential modulation, a balun is used to split the input into two out-of-phase signals, each of which drives each RM. The modulated optical signal is converted to an electrical signal by a photodetector (Coherent XPDV2320R-VF-FA) and analyzed by a RF signal analyzer (Keysight N9000B) to measure the microwave power spectrum. The photodetector output signals are amplified by an RF amplifier (SHF S807C), so that they can

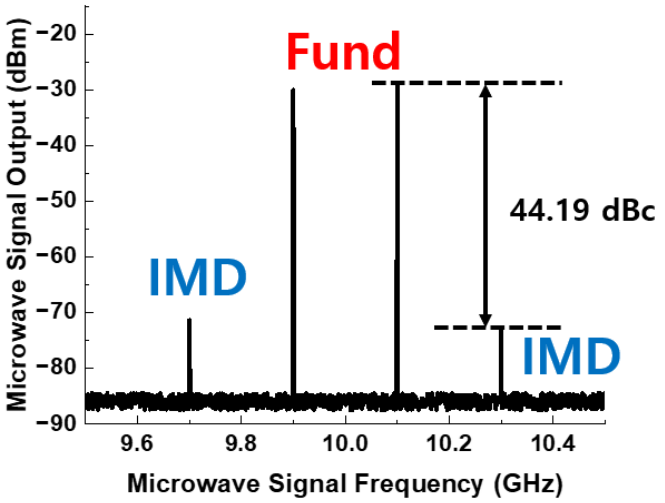

Fig. 4. Output microwave spectrum of the Si RAMZM. The input microwave signal power is 7.5 dBm. The input microwave signal frequency es are 9.9 GHz and 10.1 GHz.

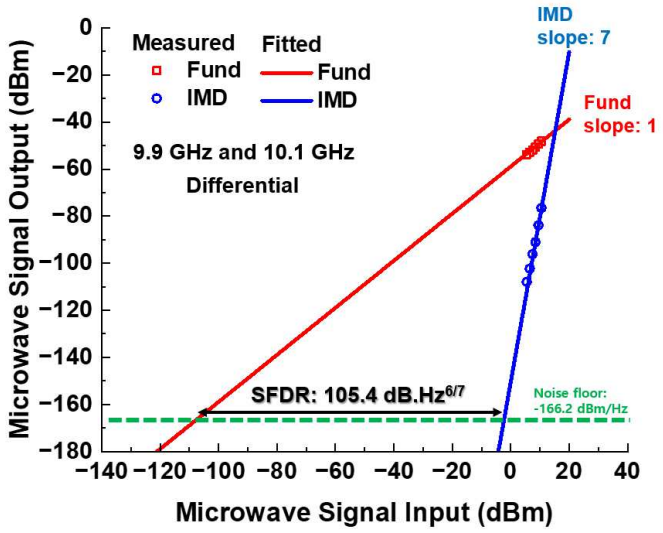

Fig. 5. Output fundamental and IMD signals along input microwave signal power. The input microwave signal frequency es are 9.9 GHz and 10.1 GHz.

be above the minimum signal level required by the signal analyzer.

Fig. 4 shows the microwave output power spectral density when the input microwave signal frequencies are 9.9 GHz and 10.1 GHz each having 7.5-dBm input power. IMD signals are shown at 9.7 GHz and 10.3 GHz.

Before determining the SFDR, the noise floor must be estimated [6]. In our measurement, when the MZI is biased at quadrature and the input wavelength is at the RM resonance, 4-dBm input light produces –5.5dBm output light, which generates 0.282 mA photocurrent. With relative intensity noise (RIN) of –140 dB/Hz for the laser used in the measurement, this corresponds to the RIN power of –167.8 dBm and the shot noise power of –172.8 dBm. With the measurement done at 25 °C, the thermal noise power is –173.9 dBm. All of these result in the noise floor of –166.2 dBm per Hz after the photodetector.

Fig. 5 shows the measured power levels of the fundamental signal and the nearest IMD components as a function of the input microwave signal power. These results show the SFDR exceeding 105 dB.Hz$^{6/7}$. The noteworthy observation is that the slope of the IMD signals is approximately 7, which indicates that the Si RAMZM nonlinearity is dominated by the 7th order. Table I compares the linearity performances of several Si photonic modulators.

TABLE I

COMPARISON OF MOULATION LINEARITY FROM SEVERAL SI EO MODULATORS

Ref.	Device structure	Device Footprint (mm^2)	Microwave Signal Frequency (GHz)	SFDR
[3]	DPMZM	5	10	127 dB.Hz$^{6/7}$
[4]	RAMZM	15	10	99 dB.Hz$^{2/3}$
[5]	RAMZM	1.38	1.1	113 dB.Hz$^{2/3}$
[7]	MZM	8	2	113.7 dB.Hz$^{2/3}$
[8]	DPMZM	6.4	10	96.5 dB.Hz$^{2/3}$
This work	RAMZM	1.02	10	105.4 dB.Hz$^{6/7}$

IV. CONCLUSION

In this work, we have designed and fabricated a Si RAMZM that exhibits high linearity of > 105-dB.Hz$^{6/7}$ SFDR at X-band with only 1-mm^2 footprint. The fabricated Si RAMZM demonstrates a slope close to 7 for the IMD component as a function of input microwave signal power, which directly contributes to the enhanced SFDR performance.

ACKNOWLEDGMENT

This work was supported by the Challengeable Future Defense Technology Research and Development Program through the ADD funded by DAPA in 2024 (UI220080TD).

REFERENCES

[1] J. Okyere, K. Yu, K. Entesari, and S. Palermo, :A fifth-order polynomial predistortion circuit for mach-zehnder modulator linearization in 65nm cmos," in *2017 Texas Symposium on Wireless and Microwave Circuits and Systems* (WMCS), IEEE, 2017, pp. 1-4.

[2] N. Hosseinzadeh, A. Jain, R. Helkey, and J. F. Buckwalter, "A distributed low-noise amplifier for broadband linearization of a silicon photonic mach-zehnder modulator," IEEE *Journal of Solid-State Circuits*, vol. 56, pp. 1897-1909, 2020.

[3] Q. Zhang, Q. Huang, P. Xia, Y. Li, X. Jiang, S. Zhang, S.Fang, J. Yang, and H.. Yu, "All-Optically Linearized Silicon Modulator with Ultrahigh SFDR of 131 dB.Hz$^{6/7}$," *Photonics Research*, vol. 13, no. 2, pp. 433–441, 2025.

[4] J. Cardenas, P. A. Morton, J. B. Khurgin, A. Griffith, C. B. Poitras, K. Preston, and M. Lipson, "Linearized silicon modulator based on a ring assisted mach zehnder inteferometer," *Optics Express*, vol. 21, pp. 22549‑22557, 2013.

[5] M. J. Shawon and V. Saexena, "Optical Linearization of Silicon Photonic Ring-Assisted Mach-Zehnder Modulator," *Journal of Lightwave Technology*, vol. 42, no. 8, pp 2868-2879, 2023.

[6] W. B. Bridges and J. H. Schaffner, "Distortion in linearized electrooptic modulators," *IEEE Transaction of Microwave Theory and Techniques*, vol. 43, no. 9, pp. 2184–2197, Sep. 1995.

[7] M. Streshinsky et al., "Highly Linear Silicon Traveling-Wave Mach–Zehnder Carrier Depletion Modulator based on Differential Drive," *Optics Express*, vol. 21, no. 3, pp. 3818–3825, 2013.

[8] Y. Zhou, L. Zhou, M. Wang, Y. Xia, Y. Zhong, and X. Li, "Linearity Characterization of a Dual–Parallel Silicon Mach–Zehnder Modulator," *IEEE Photonics Journal*, vol. 8, no. 6, Dec. 2016, Art. no. 7805108.